

A Post-Processing Scheme to Evaluate Transverse Stresses for Composite Panels under Dynamic Loads

K. Lee¹, H. Park² and S.W. Lee³

Abstract: A post-processing scheme is presented to accurately determine transverse shear and normal stresses in composite panels undergoing geometrically nonlinear deformation under dynamic loading conditions. Transverse stresses are assumed through thickness at a point of interest and are recovered via a one-dimensional finite element method. The finite element method is based on the least square functional of the error in the equilibrium equation along the thickness direction and utilizes the in-plane stresses and resultant transverse shear forces per unit length obtained by a shell element analysis. Numerical results demonstrate that, with minimal addition of computational efforts, the present post-processing approach can be used to accurately determine the time history of transverse stresses at a point of interest in composite structures under dynamic loading.

Keyword: post-processing scheme, transverse stresses, dynamic effect

1 Introduction

For multi-layered composite and sandwich structures, accurate determination of transverse stresses is prerequisite to investigation of material damage and failure. For example, any strength-based criteria for failure of composite and sandwich panels such as delamination or debonding require information on transverse stresses. Accordingly, it is desirable to have an efficient method to accurately evaluate

transverse stress distributions in the thickness direction. Analytical or semi-analytical solutions for the transverse stresses, based on the three-dimensional elasticity, have been available only for simple geometries and boundary conditions [Pagano (1970)]. Recently, Kant, Pendihari and Desai (2007) have introduced semi-analytical solutions for more general geometry and boundary conditions. However, these semi-analytical solutions are limited to geometrically linear deformation.

Within the context of the finite element method, one approach to determine the transverse stresses is to use a sufficiently large number of elements along the thickness direction. However, this approach may be impractical due to enormous computational cost, especially for cases involving geometrically nonlinear deformation under dynamic loadings. An alternative approach is to carry out the finite element analysis with a single plate or shell element through the thickness and subsequently enhance the accuracy of transverse stresses via using a post-processing scheme. An extensive literature review on the post-processing schemes, conducted by Yuan, Saleeb and Gendy (2000), reveals that most schemes have been applied to geometrically linear static cases. Several investigators [Lee and Lee (2003), Park and Kim (2003), Park, Park and Kim (2003)] have applied their schemes to geometrically nonlinear static problems. However, their applicability to geometrically nonlinear problems under dynamic loadings is still unknown.

The objective of this study is to extend a post-processing scheme, previously developed by Lee and Lee (2003) for evaluation of transverse stresses in composite panels under static loading conditions, into the cases involving dynamic load-

¹ Assistant Research Scientist, University of Maryland, College Park, MD, USA

² Senior Research Engineer, Hyundai Motor Company, Republic of Korea

³ Professor, Aerospace Engineering, University of Maryland, College Park, MD, USA

ing conditions. This post-processing scheme can handle geometrically nonlinear cases as well as linear ones. In this approach, transverse stresses are recovered via a post-processing scheme using a one-dimensional finite element method applied at a point of interest. Unknown transverse shear and normal stresses, assumed through the thickness in terms of unknown nodal values, are introduced into a least square functional based on the error in the equilibrium. The minimization of the least square functional leads to a simple linear algebraic equation, from which the unknown nodal values can be determined. Dynamic effects are incorporated into the equilibrium equation by treating the inertia force as a body force. The present post-processing scheme is based on the premises that one can accurately obtain in-plane stresses and resultant transverse shear forces per unit length via either the geometrically nonlinear finite element analysis using plate or shell elements [Park, Cho and Lee (1995), Yeom and Lee (1989), Kim and Lee (1988)] or any other methods such as the meshfree method [Han, Rajendran and Atluri (2005), Jarak, Soric and Hoster (2007), Sladek, Saldek, Wen and Aliabadi (2006), Wen and Hon (2007)]. For the finite element method, it is known that inplane stresses are accurate at the superconvergent stress points in an element and various recovery techniques are available for accurate determination of inplane stresses at other points [Zienkiewicz and Zhu (1992), Lee, Park and Lee (1997)].

2 Formulation for stress recovery

The equilibrium equations for solids, undergoing geometrically nonlinear deformation, can be expressed as

$$\frac{\partial \mathbf{S}_x}{\partial x} + \frac{\partial \mathbf{S}_y}{\partial y} + \frac{\partial \mathbf{S}_z}{\partial z} + \mathbf{F}_B = 0 \quad (1)$$

where \mathbf{F}_B is the body force vector, and \mathbf{S}_x , \mathbf{S}_y , \mathbf{S}_z are the 2nd Piola-Kirchhoff stress vectors which

can be expressed as

$$\begin{aligned} \mathbf{S}_x &= S_{xx} \frac{\partial \mathbf{R}}{\partial x} + S_{xy} \frac{\partial \mathbf{R}}{\partial y} + S_{xz} \frac{\partial \mathbf{R}}{\partial z} \\ \mathbf{S}_y &= S_{yx} \frac{\partial \mathbf{R}}{\partial x} + S_{yy} \frac{\partial \mathbf{R}}{\partial y} + S_{yz} \frac{\partial \mathbf{R}}{\partial z} \\ \mathbf{S}_z &= S_{zx} \frac{\partial \mathbf{R}}{\partial x} + S_{zy} \frac{\partial \mathbf{R}}{\partial y} + S_{zz} \frac{\partial \mathbf{R}}{\partial z} \end{aligned} \quad (2)$$

where S_{xx}, \dots, S_{zz} are the 2nd Piola-Kirchhoff stress components, and \mathbf{R} is the position vector in the deformed configuration. The position vector \mathbf{R} can be expressed as

$$\mathbf{R} = \begin{Bmatrix} x + u \\ y + v \\ z + w \end{Bmatrix} \quad (3)$$

where u, v, w are the displacements along x, y, z direction, respectively. The body force vector due to the inertia forces can be expressed as

$$\mathbf{F}_B = \begin{Bmatrix} -\rho \ddot{u} \\ -\rho \ddot{v} \\ -\rho \ddot{w} \end{Bmatrix} \quad (4)$$

where ρ is the mass per unit volume and $\ddot{u}, \ddot{v}, \ddot{w}$ are the accelerations of the solids along the x, y, z directions, respectively. Using the indicial notation, one can express the k -th component ($k = 1, 2, 3$) of the equilibrium equations Q_k as

$$\begin{aligned} Q_k &= \sum_{i=1}^3 \sum_{j=1}^3 \left[\frac{\partial S_{ij}}{\partial x_i} \left(\delta_{jk} + \frac{\partial u_k}{\partial x_j} \right) + S_{ij} \frac{\partial^2 u_k}{\partial x_i \partial x_j} \right] - \rho \ddot{u}_k \\ &= 0 \end{aligned} \quad (5)$$

where δ_{jk} is the Dirac delta function and displacements u_1, u_2, u_3 correspond to u, v, w respectively. The left hand side of the equation (5) can be divided into two parts as follows:

$$Q_k = Q_{k1} + Q_{k2} \quad (6)$$

where Q_{k1} represents a known part and Q_{k2} is an unknown part. We assume that the in-planes stress terms and the inertia force terms are accurately obtained by the results of the shell element analysis. Accordingly, the known part can be written

in terms of in-plane stresses and the inertia forces only. The unknown part is composed of the transverse stress terms that are to be determined. The known part of equation (5) can be expressed as

$$Q_{k1} = \sum_{i=1}^2 \sum_{j=1}^2 \left[\frac{\partial S_{ij}}{\partial x_i} \left(\delta_{jk} + \frac{\partial u_k}{\partial x_j} \right) + S_{ij} \frac{\partial^2 u_k}{\partial x_i \partial x_j} \right] - \rho \ddot{u}_k \quad (7)$$

All remaining terms constitute the unknown part, which can be expressed as

$$\begin{aligned} Q_{k2} = & \left(\frac{\partial S_{13}}{\partial x_1} + \frac{\partial S_{23}}{\partial x_2} + \frac{\partial S_{33}}{\partial x_3} \right) \left(\delta_{3k} + \frac{\partial u_k}{\partial x_3} \right) \\ & + \left(\frac{\partial S_{31}}{\partial x_3} \right) \left(\delta_{1k} + \frac{\partial u_k}{\partial x_1} \right) \\ & + \left(\frac{\partial S_{32}}{\partial x_3} \right) \left(\delta_{2k} + \frac{\partial u_k}{\partial x_2} \right) \\ & + S_{13} \frac{\partial^2 u_k}{\partial x_1 \partial x_3} + S_{23} \frac{\partial^2 u_k}{\partial x_2 \partial x_3} + S_{31} \frac{\partial^2 u_k}{\partial x_3 \partial x_1} \\ & + S_{32} \frac{\partial^2 u_k}{\partial x_3 \partial x_2} + S_{33} \frac{\partial^2 u_k}{\partial x_3^2} \end{aligned} \quad (8)$$

The procedure for stress recovery can be described via expressing the transverse stresses assumed in the thickness direction as follows:

$$S_{xz} = \mathbf{N}_{xz} \mathbf{x}_1, \quad S_{yz} = \mathbf{N}_{yz} \mathbf{x}_2, \quad S_{zz} = \mathbf{N}_{zz} \mathbf{x}_3 \quad (9)$$

where $\mathbf{N}_{xz}, \mathbf{N}_{yz}, \mathbf{N}_{zz}$ are the row vectors of assumed shape functions and $\mathbf{x}_1, \mathbf{x}_2, \mathbf{x}_3$ are the corresponding vectors of unknown nodal values along the thickness direction.

With the use of equation (9), $\boldsymbol{\varepsilon}$, the error of the equilibrium equation (1), can be symbolically expressed in matrix form as follows.

$$\boldsymbol{\varepsilon} = \frac{\partial \mathbf{S}_x}{\partial x} + \frac{\partial \mathbf{S}_y}{\partial y} + \frac{\partial \mathbf{S}_z}{\partial z} - \rho \ddot{\mathbf{u}} = (\mathbf{A}\mathbf{x} - \mathbf{b}) \quad (10)$$

where matrix \mathbf{A} and column vector \mathbf{b} are known quantities and \mathbf{x} is the vector of unknown nodal values of the assumed transverse stresses. The unknown \mathbf{x} vector can be determined by minimizing the least square functional based on the error of

equilibrium equation defined as follows:

$$\begin{aligned} L(\mathbf{x}) &= \int (\boldsymbol{\varepsilon}^T \cdot \boldsymbol{\varepsilon}) dz \\ &= \int (\mathbf{A}\mathbf{x} - \mathbf{b})^T (\mathbf{A}\mathbf{x} - \mathbf{b}) dz \end{aligned} \quad (11)$$

Note that the integration is through the thickness only. The minimization condition of $L(\mathbf{x})$ with respect to \mathbf{x} leads to

$$\left[\int (\mathbf{A}^T \mathbf{A}) dz \right] \mathbf{x} = \int (\mathbf{A}^T \mathbf{b}) dz \quad (12)$$

or

$$\mathbf{K}\mathbf{x} = \mathbf{f} \quad (13)$$

where

$$\begin{aligned} \mathbf{K} &= \int (\mathbf{A}^T \mathbf{A}) dz \\ \mathbf{f} &= \int (\mathbf{A}^T \mathbf{b}) dz \end{aligned} \quad (14)$$

In the finite element approximation, one-dimensional elements are introduced along the thickness and the \mathbf{K} and \mathbf{f} are assembled from the element values. For this, the least square functional can be expressed as

$$\begin{aligned} L(\mathbf{x}) &= \sum_{e=1}^N \left[\int_e \boldsymbol{\varepsilon}_e^T \cdot \boldsymbol{\varepsilon}_e dz \right] \\ &= \sum_{e=1}^N \left[\int_e (\mathbf{A}_e \mathbf{x}_e - \mathbf{b}_e)^T (\mathbf{A}_e \mathbf{x}_e - \mathbf{b}_e) dz \right] \end{aligned} \quad (15)$$

where $\boldsymbol{\varepsilon}_e$ is the error of the equilibrium equation within the element expressed as

$$\boldsymbol{\varepsilon}_e = \left(\frac{\partial \mathbf{S}_x}{\partial x} + \frac{\partial \mathbf{S}_y}{\partial y} + \frac{\partial \mathbf{S}_z}{\partial z} - \rho \ddot{\mathbf{u}} \right)_{\text{element}} \quad (16)$$

The \mathbf{K} matrix and \mathbf{f} vector can be expressed with the quantities defined in each element as follows:

$$\begin{aligned} \mathbf{K} &= \sum_{e=1}^N \int_e (\mathbf{A}_e^T \mathbf{A}_e) dz = \sum_{e=1}^N \mathbf{K}_e \\ \mathbf{f} &= \sum_{e=1}^N \int_e (\mathbf{A}_e^T \mathbf{b}_e) dz = \sum_{e=1}^N \mathbf{f}_e \end{aligned} \quad (17)$$

The unknown \mathbf{x} vector is determined by solving equation (13). As shown in equations (7) and (8), the current scheme requires the information on the in-plane derivatives of in-plane stresses as well as the in-plane derivatives of the transverse shear stresses. The in-plane stress derivatives can be obtained by using the stress values at the superconvergent stress points of the elements that share common boundaries with the element that contains the point of interest at which the transverse stresses are being recovered [Lee and Lee 2003]. On the other hand, the derivatives of the transverse shear stresses can be obtained using the following equations:

$$\frac{\partial S_{xz}}{\partial x} = \frac{\partial Q_x}{\partial x} \frac{S_{xz}}{Q_x} \quad (18)$$

$$\frac{\partial S_{yz}}{\partial y} = \frac{\partial Q_y}{\partial y} \frac{S_{yz}}{Q_y} \quad (19)$$

where Q_x and Q_y are the resultant transverse shear forces per unit length computed from the analysis using a shell finite element model or a meshless method. One may refer to Lee and Lee [2003] for additional details on the implementation of the current scheme.

3 Numerical examples

Numerical tests are conducted to evaluate the validity and effectiveness of the present post-processing scheme to determine the transverse stresses under dynamic loading conditions. The structures chosen for test are laminated composite plates under uniform pressure loads, either constant or triangular in time. The nine-node assumed strain solid shell elements are used to generate the displacement, in-plane stresses and resultant transverse shear forces per unit length that are needed as the input to the stress recovery scheme described in the present paper. As for the unknown transverse stresses, the transverse shear stresses are assumed to be quadratic while the transverse normal stress is assumed cubic in an element. Twelve one-dimensional elements are used through the thickness at a selected point of interest.

3.1 A clamped composite plate under uniform step function pressure loads

The first example chosen for test is a laminated composite plate with all four edges clamped, subjected to uniform transverse pressure load in step input form initiated at $t = 0$. The material properties of the composite panel are shown in Table 1, and the geometrical data and lay-up sequence are given in Table 2.

Table 1: Mechanical properties of laminate composite

Longitudinal Modulus, E_1	43.34 GPa
Transverse Modulus, E_2	12.73 GPa
Shear Modulus, G_{12}	4.46 GPa
Poisson's Ratio, ν_{12}	0.29
Density, ρ	1800 kg/m ³

Table 2: Ply lay-up and geometrical dimensions of the plate

Lay-Up Sequence	No. of Plies	Length (mm)	Width (mm)	Thickness (mm)
$[0/90]_S$	4	220	220	3.43

As shown in Fig. 1, utilizing the symmetry in geometry and loading, the left upper quarter of the plate is chosen for finite element analysis with fourteen elements in the length and the width directions.

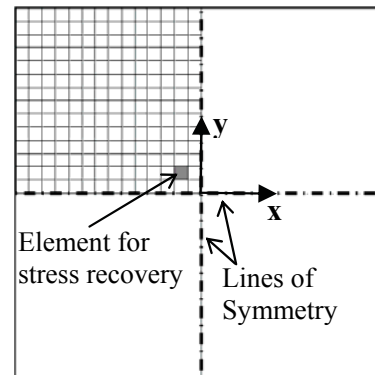


Figure 1: Analysis region and location of the element of interest

Geometrically nonlinear dynamic analyses are carried out under a step loading of uniform pressure of 1.0 kPa and 100.0 kPa. Subsequently, the transverse stresses are evaluated via the present post-processing approach at the center of the shaded element as shown in Figure 1.

Figures 2 and 3 show the time histories of the normal displacement at the center of plate. As shown in the figures, due to the geometrically nonlinear effect, the amplitude is not proportional to the magnitude of the applied load. For the pressure load of 100.0 kPa, the maximum displacement is about 1.3 times the plate thickness.

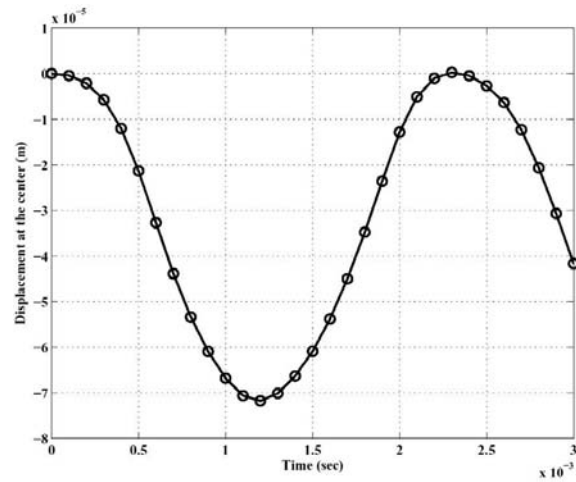


Figure 2: Center displacement vs. time for $p = 1$ kPa

Figures 4 and 5 show the six stress components at three locations through the thickness direction obtained by using the 14x14 mesh and time increment $\Delta t = 1.0 \times 10^{-4}$ (sec). In these figures the z coordinate is normal to the plate with $z = 0$ at the midplane and t is the plate thickness. The three in-plane stresses are the direct result of the finite element analysis using the solid shell element. For the higher pressure of 100 kPa, the asymmetries in the inplane stresses through the thickness are highly pronounced due to geometrically nonlinear behavior of the composite plate. As for the transverse stresses, we observe that their maximum values are very small relative to those of the inplane normal stresses.

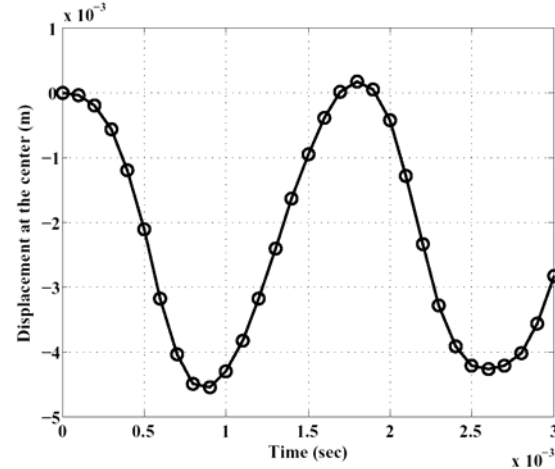


Figure 3: Center displacement vs. time for $p = 100$ kPa

3.2 A clamped plate under time-varying pressure loads

In this example, a laminated composite plate is subjected to a dynamic pressure load which is uniform over the plate surface but is in the form of two triangular shapes in time. The material properties for the composite plate are shown in Table 1, and the geometrical data and lay-up sequence are given in Table 3. Figure 1 shows the composite plate, clamped along the four edges. Due to the symmetry in geometry and loading, only the left upper quarter of the plate is chosen for finite element analysis with a mesh of 14x14 elements.

Table 3: Ply lay-up and geometrical dimensions of the plate

Lay-Up Sequence	No. of Plies	Length (mm)	Width (mm)	Thickness (mm)
$[0/90]_S$	4	440	440	3.43

The applied pressure is assumed vary in time as follows:

$$P(t) = \begin{cases} 2P_{max} \frac{t}{T} & 0 \leq t < \frac{T}{2} \\ 2P_{max} (1 - \frac{t}{T}) & \frac{T}{2} \leq t \leq T \end{cases} \quad (20)$$

where the two parameters P_{max} and T determine one cycle of the triangular dynamic pressure loading. Two cycles of dynamic loading with P_{max}

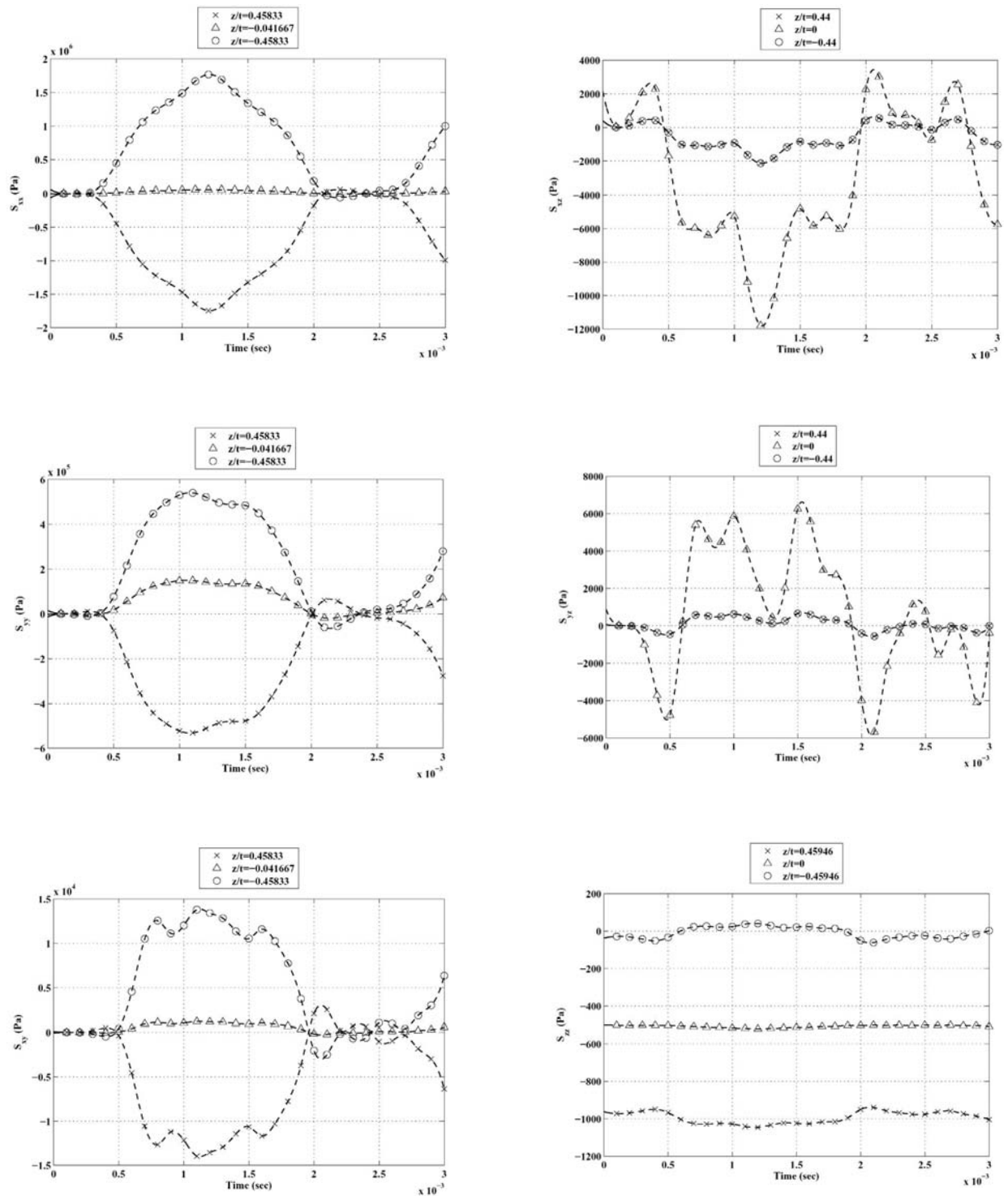


Figure 4: Stress components vs. time at three different locations through the thickness (14x14 mesh, $p = 1$ kPa, $\Delta t = 1.0 \times 10^{-4}$ (sec))

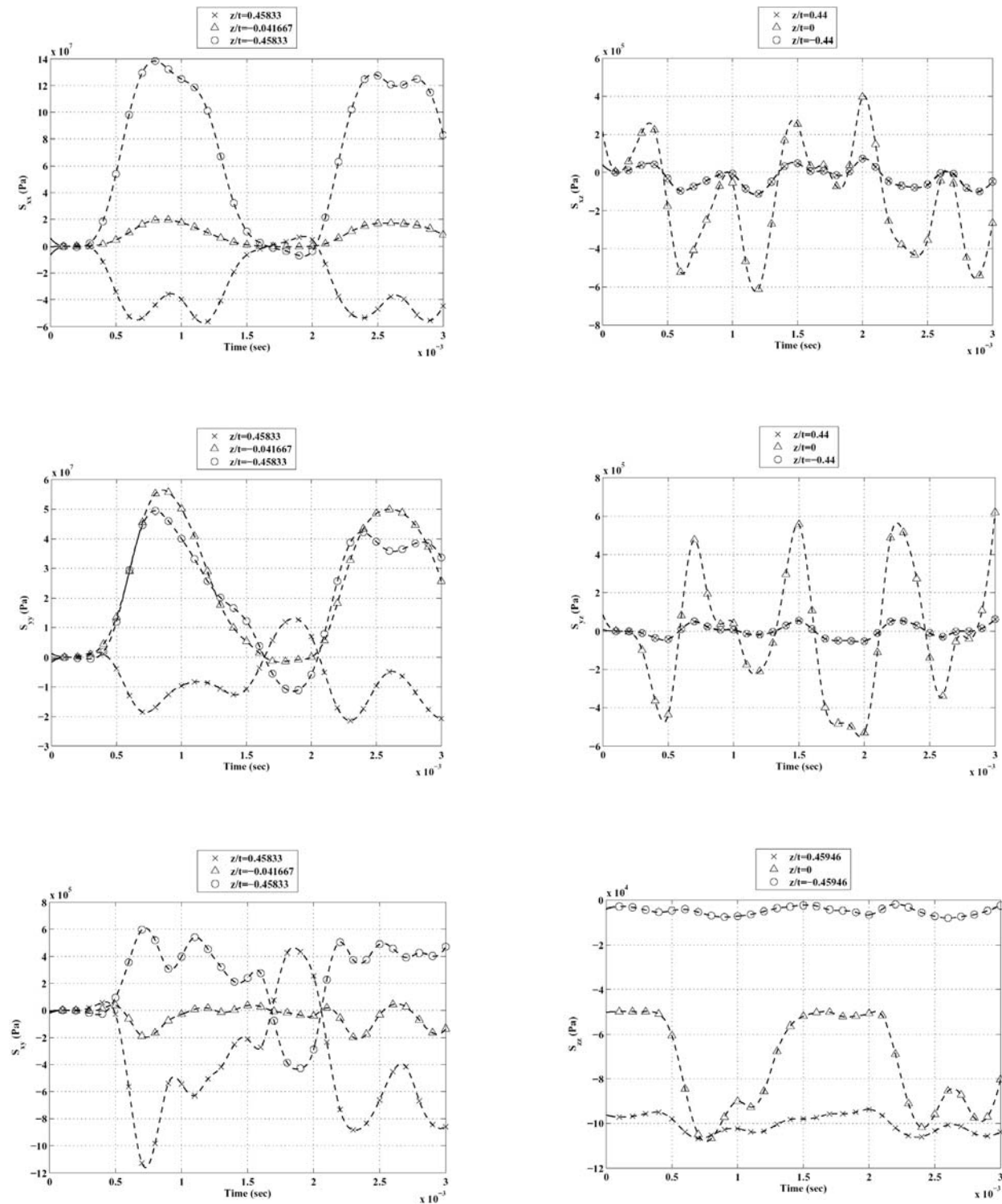


Figure 5: Stress components vs. time at three different locations through the thickness (14×14 mesh, $p = 100$ kPa, $\Delta t = 1.0 \times 10^{-4}$ (sec))

= 0.1 MPa and $T = 1/150$ second are applied as shown in Figure 6. Geometrically nonlinear dynamic analyses are carried out and subsequently the transverse stresses are evaluated at a selected point of interest via using the present post-processing approach.

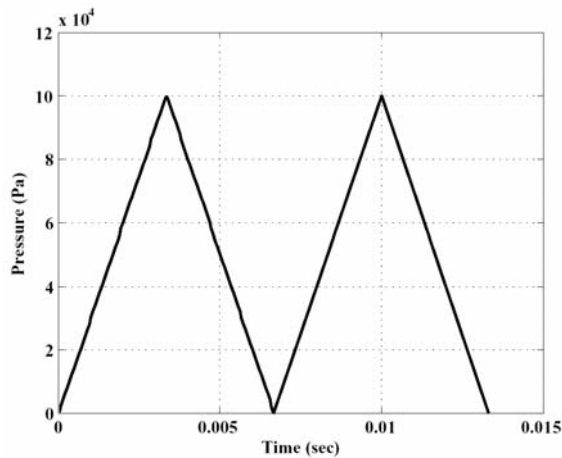


Figure 6: Pressure vs. time for the triangular dynamic pressure loading

Figure 7 shows the time history of the transverse displacement at the plate center. As shown in the figure, the maximum displacement is more than four times the plate thickness.

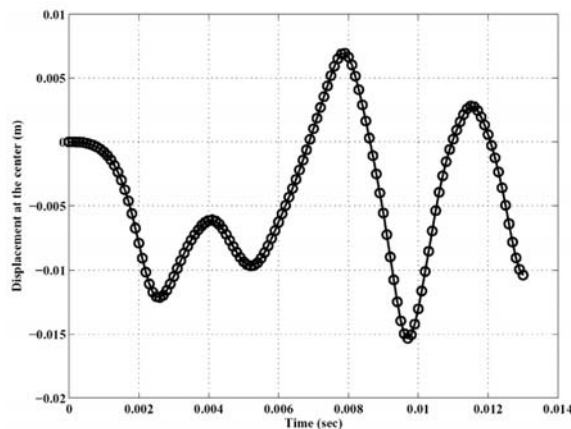


Figure 7: Center displacement vs. time for the triangular dynamic pressure loading

Figure 8 shows the stress components vs. time at the three different locations through the thickness. The stresses are evaluated at the center of

the shaded element shown in Fig. 1. The in-plane stresses, which are obtained directly from the geometrically nonlinear dynamic analyses, are highly asymmetric through the thickness due to geometrically nonlinear nature of the deformation. Once again, we observe that the maximum values of the transverse stresses are very small compared with the maximum inplane normal stress values.

4 Conclusions

The results of numerical tests demonstrate the validity and effectiveness of the present post-processing scheme to recover transverse stresses of geometrically nonlinear composite panels under dynamic loading conditions. The present approach is attractive in that the transverse stresses are evaluated only at a point of interest at a given instant in time via utilizing a one-dimensional finite element method along the thickness direction. Accordingly, the scheme requires minimal computational effort, when used to determine transverse stresses in composite panels undergoing geometrically nonlinear deformation subjected to dynamic loadings. Moreover, the scheme is equilibrium-based and is independent of constitutive behavior of the structural material.

Acknowledgement: This research was sponsored by the Office of Naval Research as well as the U.S. Army Research Laboratory (ARL) at the Aberdeen Proving Ground, MD. For the ARL, late Dr. Ki Kim of the Survivability/Lethality Analysis Directorate was the technical monitor. Authors would like to thank Dr. Jihan Kim for his technical help.

References

- Han, Z.D.; Rajendran, A.M.; Atluri, S.N.** (2005): Meshless Local Petrov-Galerkin (MLPG) Approaches for Solving Nonlinear Problems with Large Deformations and Rotations, *CMES: Computer Modeling in Engineering & Sciences*, Vol. 10, Num. 1, pp. 1-12.
- Jarak, T.; Soric, J.; Hoster, J.** (2007): Analysis of Shell Deformation Responses by the Meshless Local Petrov-Galerkin (MLPG) Approach,

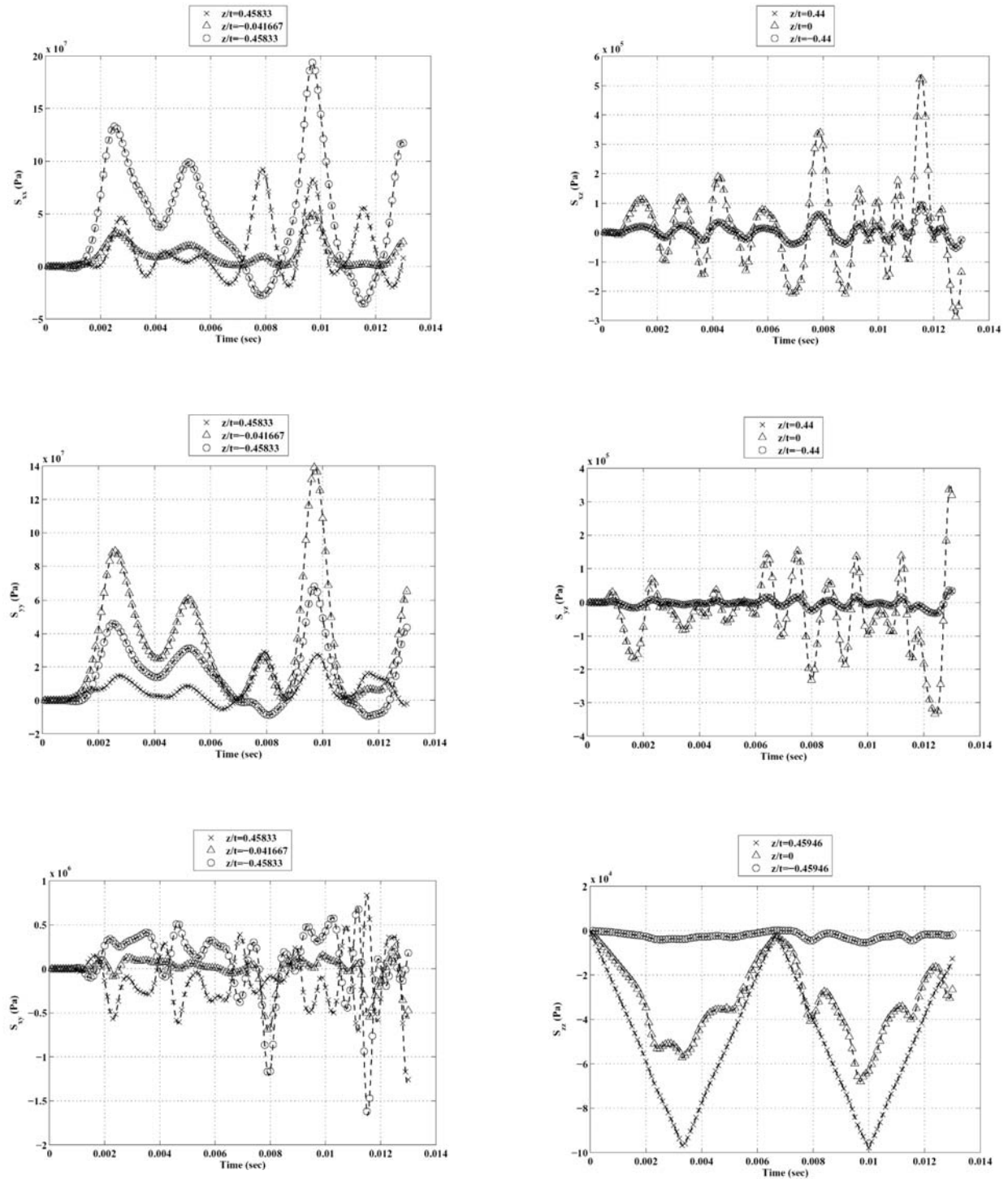


Figure 8: Stress components vs. time at three different locations through the thickness (14×14 mesh, $\Delta t = 1.0 \times 10^{-4}$ (sec))

CMES: Computer Modeling in Engineering & Sciences, Vol. 18, Num. 3, pp. 235-246.

Kant, T.; Pendhari, S.S.; Desai, Y.M. (2007): A General Partial Discretization Methodology for Interlaminar Stress Computation in Composite Laminates, *CMES: Computer Modeling in Engineering & Sciences*, Vol. 17, Num. 2, pp. 135-161.

Kim, Y.H.; Lee, S.W. (1988): A Solid Element Formulation for Large Deflection Analysis of Composite Shell Structures, *Computers and Structures*, Vol. 30, pp. 269-274.

Lee, K.; Lee, S.W. (2003): A Post-Processing Approach to Determine Transverse Stress in Geometrically Nonlinear Composite and Sandwich Structures, *Journal of Composite Materials*, Vol. 37, Num 24, pp. 2207-2224.

Lee, T.O.; Park, H.C.; Lee, S.W. (1997): 'A Superconvergent Stress Recovery Technique with Equilibrium Constraint,' *International Journal for Numerical Methods in Engineering.*, Vol. 40, Num. 7, pp.1139-1160.

Pagano, N.J. (1970): Exact Solutions for Rectangular Bidirectional Composites and Sandwich Plates, *Journal of Composite Materials*, Vol. 4, pp. 20-34.

Park, B.C.; Park, J.W.; Kim, Y.H. (2003): Stress Recovery in Laminated Composite and Sandwich Panels Undergoing Finite Rotation, *Composite Structures*, Vol. 59, Num 2, pp. 227-235.

Park, H.C.; Cho, C.M.; Lee, S.W. (1995): An Efficient Assumed Strain Element Model with Six DOF per Node for Analysis of Geometrically Nonlinear Shells, *International Journal for Numerical Methods in Engineering*, Vol. 38, Num. 24, pp. 4101-4121.

Park, J.W.; Kim, Y.H. (2003): Local Recovery of Through-The-Thickness Stresses in Laminated Composite Plates, *Composite Structures*, Vol. 59, Num. 2, pp. 291-296.

Sladek, J.; Saldek, V.; Wen, P.H.; Aliabadi, M.H. (2006): Meshless Local Petrov-Galerkin (MLPG) Method for Shear Deformable Shells Analysis, *CMES: Computer Modeling in Engineering and Sciences*, Vol. 13, Num. 2, pp. 103-

117.

Yeom, CH; Lee, SW (1989): An Assumed Strain Element Model for Large Deflection Composite Shells, *International Journal of Numerical Methods in Engineering*, Vol. 28, pp. 1749-1768.

Yuan, J.; Saleeb, A.; Gendy, A. (2000): Stress Projection, Layerwise-Equivalent, Formulation for Accurate Predictions of Transverse Stresses in Laminated Plates and Shells, *International Journal of Computational Engineering Science*, Vol. 1, Num. 1, pp. 91-138.

Wen, P.H.; Hon, Y.C. (2007): Geometrically Nonlinear Analysis of Reissner-Mindlin Plate by Meshless Computation, *CMES: Computer Modeling in Engineering & Sciences*, Vol. 21, Num. 3, pp. 171-191.

Zienkiewicz, O.C.; Zhu, J.Z. (1992): The Super-Convergent Patch Recovery and a Posteriori Error Estimates. Part 1: The Recovery Technique, *International Journal for Numerical Methods in Engineering*, Vol. 33, pp. 1331-1364.